Simulation Results of Compressible Unsteady Flows Using the Quasi-3D Method

Victor GHEORGHIU
Department of Mechanical Engineering
University of Applied Sciences Hamburg, Germany
E-mail: grg@rzbt.haw-hamburg.de

Abstract

The purpose of this paper is to present some simulation results by means of the **quasi-3D method** of the compressible unsteady flow of a viscous fluid through pipes and manifolds of internal combustion engines (ICE). The quasi-3D method can describe the influence of the gas flow three-dimensionality correctly (i.e. curvatures, asymmetry of the pipes and channels etc.), that improves the simulation quality noticeably (compared to the classical 1D-simulation) without increasing the cost of computation proportionally (compared to the classical 3D-simulation). Apart from some theoretical basics, the quasi-3D method is applied (as an example) to a one-cylinder research diesel engine. The comparison between simulation results in intake pipe and pressure measurements in multi-point intake pipe at some engine speeds and two loads is shown and commented.

INTRODUCTION

The design of intake and exhaust ICE manifolds has been an important application of unsteady fluid dynamics for many years. A first purpose of these simulations is the optimizing of the cylinder filling, the accordance with the turbocharger etc. about wide load and engine speed intervals. A second purpose is the estimating of the required initial conditions for the simulation of the in cylinder air/fuel mixture formation and burning processes, which must have knowledge about the quantity, the composition and the flow-field of the intake charge.

Since the computation costs are high for the implementation of unsteady three-dimensional (3D) simulations of the gas exchange processes usual one-dimensional (1D) simulations are used instead. In this case, since the 1D-simulation of the gas flow processes cannot describe the whole reality (i.e. the three-dimensionality) of the gas flow correctly, curvatures, asymmetry of the pipes and channels in the simulation are disregarded.

In order to find a compromise procedure for this situation, the **quasi-3D method** [3], [4] is used. This method is based on the 1D partial differential equations (PDEs), which models the unsteady compressible flow process of a viscous fluid.

PRESENTATION OF THE QUASI-3D PDEs

For the theoretical development of the 1D PDEs it is helpful to use the stream thread notion. In this case, the lateral surface of the stream thread is impermeable to matter, since this area itself is formed by streamlines. The classical stream thread notion is generally characterized as follows: *The variations of all state variables in the cross direction of a stream thread are much lower than in its longitudinal direction* [8]. The quasi-3D stream thread notion supplements the classical one by accepting that the *flow velocity varies significant in the cross direction too* [3], [4].

In case of a pipe flow, since the tube wall (similar to the stream thread lateral surface) is impermeable to matter, the quasi-3D stream thread notion can be put into practice perfectly. This notion has the advantage that one can take into account the effect of the interior curvatures, asymmetry etc. of the pipes and channels on the resulting distorted velocity field.

The 3D flow equations are deduced appropriately, as to consider the distortion of the velocity distribution (size and direction) in each quasi-3D stream thread (pipe) cross-section. Their integration over the pipe cross-section results in the 1D flow equations, the terms of which still contain integrals of the velocity distribution. These integrals are designated as **adjustment coefficients** of the 1D flow, since they describe the 3D distribution of the gas flow velocity. The 1D flow equations together with the adjustment coefficients (5), (6), (7) form the **quasi-3D PDEs** (1) [3], [4].

The adjustment coefficients α, β (known as *Coefficient of Boussinesq* [1], [2]) and γ are treated as temporally independent parameters in each pipe cross-section.

Symbols

ρ	= gas density
p	= gas pressure
κ	= gas isentropic exponent
r_i	= mass fraction of the gas component i (for ex. of the exhaust gas)
A	= pipe cross-section
v	= local flow velocity
c	= local axial flow velocity
C	= average value of c over A (s. definition (8))
α, β, γ	= adjustment coefficients
λ_D	= wall friction coefficient
R_G	= gas constant (ideal gas)
D_H	= pipe hydraulic diameter
k	= heat transfer coefficient
T	= gas temperature
T_W	= pipe wall temperature
ζ	= loss coefficient

Indices

t, x	= partial differentiation with respect to time t or to space x

$$\boldsymbol{U}_t + \boldsymbol{F}(\boldsymbol{U})_x = \boldsymbol{H}(\boldsymbol{U}) \tag{1}$$

$$\boldsymbol{U} = \begin{bmatrix} \rho \\ \rho \cdot C \\ \dfrac{p}{\kappa - 1} + \gamma \cdot \dfrac{\rho \cdot C^2}{2} \\ r_i \cdot \rho \end{bmatrix} = \begin{bmatrix} U_1 \\ U_2 \\ U_3 \\ U_4 \end{bmatrix} \tag{2}$$

$$\boldsymbol{F}(\boldsymbol{U}) = \begin{bmatrix} U_2 \\ (\kappa - 1) \cdot U_3 + \left(\beta - \dfrac{\kappa - 1}{2} \cdot \gamma\right) \cdot \dfrac{U_2^2}{U_1} \\ \dfrac{U_2}{U_1} \cdot \left(\kappa \cdot U_3 + \dfrac{\alpha - \kappa \cdot \gamma}{2} \cdot \dfrac{U_2^2}{U_1}\right) \\ \dfrac{U_2}{U_1} \cdot U_4 \end{bmatrix} \tag{3}$$

$$\boldsymbol{H}(\boldsymbol{U}) = \begin{bmatrix} -U_1 \cdot \left(\dfrac{A_t}{A} + \dfrac{U_2}{U_1} \cdot \dfrac{A_x}{A}\right) \\ -U_2 \cdot \left[\left(\dfrac{A_t}{A} + \beta \cdot \dfrac{U_2}{U_1} \cdot \dfrac{A_x}{A}\right) + \dfrac{1}{2} \cdot \dfrac{\lambda_D}{D_H} \cdot \dfrac{|U_2|}{U_1}\right] \\ H_3 \\ -U_4 \cdot \left(\dfrac{A_t}{A} + \dfrac{U_2}{U_1} \cdot \dfrac{A_x}{A}\right) \end{bmatrix} \tag{4}$$

with

$$H_3 = \left[-\left(\frac{A_t}{A} + \kappa \cdot \frac{U_2}{U_1} \cdot \frac{A_x}{A}\right) - \frac{4 \cdot k}{D_H} \cdot \frac{\kappa - 1}{U_1 \cdot R_G}\right] \cdot \left(U_3 - \frac{\gamma}{2} \cdot \frac{U_2^2}{U_1}\right) - \frac{1}{2} \cdot \frac{U_2^2}{U_1} \cdot \left[\left(\gamma \cdot \frac{A_t}{A} + \alpha \cdot \frac{U_2}{U_1} \cdot \frac{A_x}{A}\right) - \frac{\lambda_D}{D_H} \cdot \frac{|U_2|}{U_1}\right] + \frac{4 \cdot k}{D_H} \cdot T_W$$

INTEGRATION OF THE QUASI-3D PDEs

For the integration of the quasi-3D PDEs (as example) the finite-difference method with the so-called total variation diminishing method, Lax-Friedrichs non-MUSCL (monotonic upstream schemes approach) for the homogeneous PDEs (i.e. without source terms) is used [7], [3], [4]. In order to consider the effect of the source terms from the vector ***H***, the TVD technique is integrated in a predictor-corrector procedure [7], [3], [4].

$$\alpha = \frac{1}{C^3 \cdot A} \cdot \int_{A(t)} v^2 \cdot c \cdot dA \qquad (5)$$

$$\beta = \frac{1}{C^2 \cdot A} \cdot \int_{A(t)} c^2 \cdot dA \qquad (6)$$

$$\gamma = \frac{1}{C^2 \cdot A} \cdot \int_{A(t)} v^2 \cdot dA \qquad (7)$$

$$C = \frac{1}{A} \cdot \int_{A(t)} c \cdot dA \qquad (8)$$

PRESENTATION OF THE SIMULATION RESULTS AND THEIR COMPARISON WITH THE MEASUREMENTS

For validating of the simulation results an AVL 520 one-cylinder research engine of the laboratory for Power Engineering, Piston and Turbo Machines of the University of Applied Sciences Hamburg was used. The arrangement of all measuring points is represented in the Figure 1.

Figure 2 shows the computing mesh of the intake pipe and intake port segment, i.e., between the intake silencer and the inlet valve. Figure 3 shows only the computing mesh of the intake channel with relative pressure und flow velocity vectors (only in 10x10 resampling Cartesian grid) distributions in some (perpendicular to x-axis and 30 mm spaced) sections.

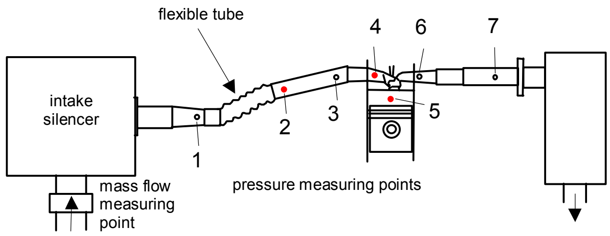

Fig. 1 Arrangement of all measuring points

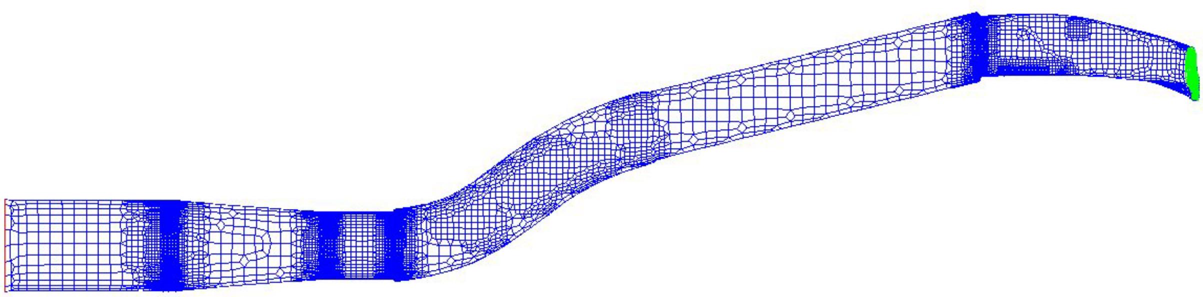

Fig. 2 Computing mesh of the all intake pipe

These simulations of the steady turbulent compressible airflow - carry out with the CFD program FIRE - are accomplished only for a compressible turbulent steady forward and reverse airflow through the intake pipe and inlet port.

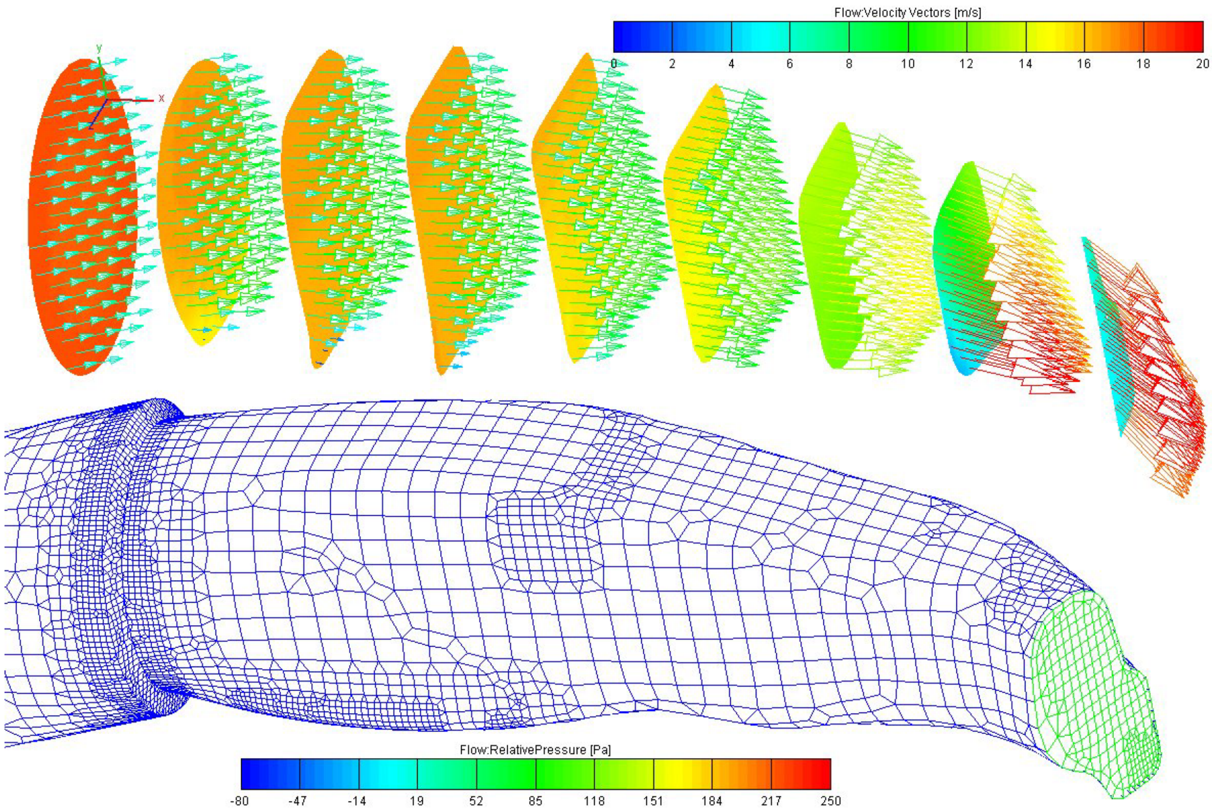

Fig. 3 Intake channel computing mesh with relative pressure und flow velocity vectors distributions in some sections by 0.03 kg/s forward mass airflow

For computing of the adjustment coefficients α, β and γ variations, i.e. for computing of the integrals from (5) to (8), the simulation results from FIRE are exported and with MATLAB post-processed.

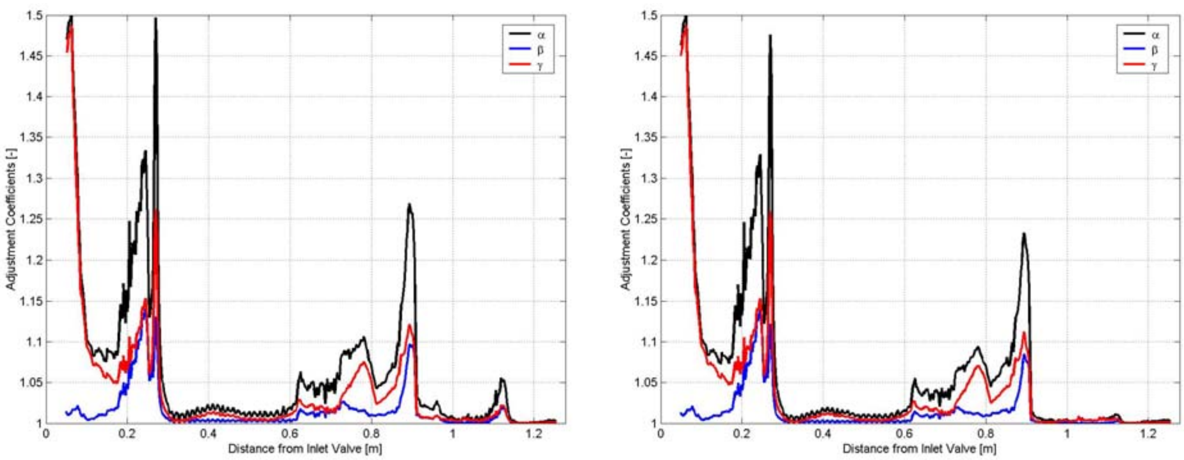

Fig. 4 Adjustment coefficient distributions by 0.01 (left) and 0.03 kg/s forward mass airflow over the **distance from the inlet valve** (mirror representation regarding Fig. 2 and 3, i.e. the airflow is directed here from right to left)

On must test first, if the hypothesis *the height of the mass flow has now influence over the adjustment coefficients height and distribution* works. Figure 4 shows these distributions by 0.01 and 0.03 kg/s forward mass airflow. On remarks that the differences are negligible and consequently this hypothesis is justified.

In the case of the reverse flow is the situation differently. The comparison between forward (Figure 4 right) and backward (Figure 5 right) 0.01 kg/s mass airflow shows practical other distribution and other height for the adjustment coefficients.

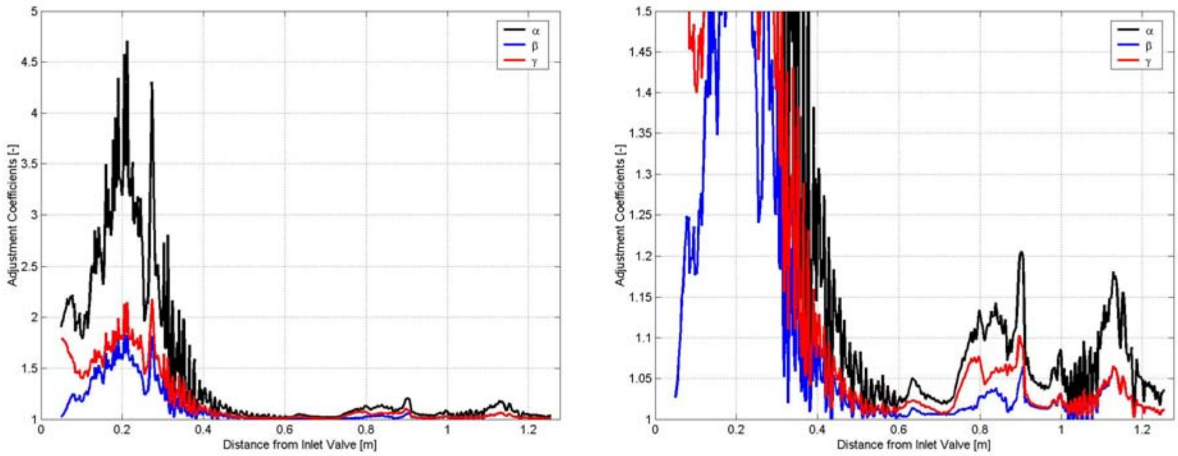

Fig. 5 Adjustment coefficient distributions by 0.01 kg/s backward mass airflow (right with the same scale like in Fig. 4) over the **distance from the inlet valve**

The quasi-3D method can be applied now to the simulation of the gas exchange processes. The simulation results and the pressure measurements are presented here only in some engine operating points (s. Figure 6). Along of the intake pipe (apart of the junction between silencer and this pipe were $\zeta = 0.14$) no other local loss coefficients are used in this case. The analysis of the pressure variations at the measuring points shows quite good agreement between simulations and experiments.

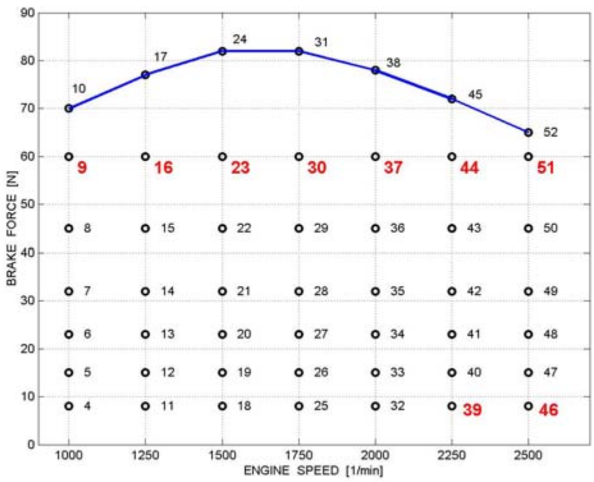

Fig. 6 Engine operating points map

In the Figures 8 to 16 only the pressure variations comparison at the measuring points 2 and 4 at seven engine speeds and two loads (s. EOPs from Figure 6) are presented. Presented supplementary are the pressure, flow speed, density and exhaust gas mass fraction (EGMF) variations as 3D-diagrams, i.e. as isometric illustrations in the distance-crank angle (distance-time) plane. In all these 3D-diagrams, the surfaces of these state variables are presented according to the notations from Figure 7.

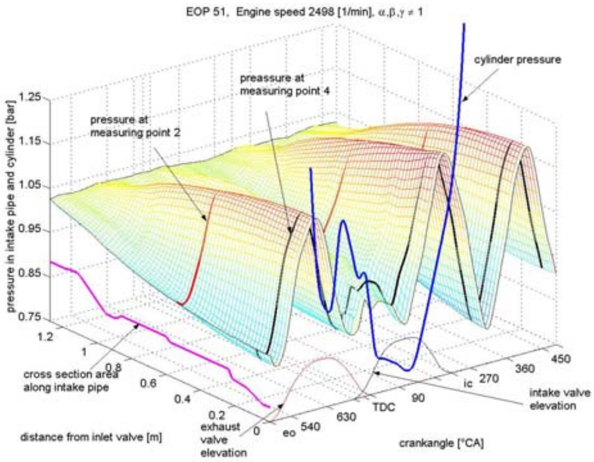

Figure 7 3D-diagram of a state variable in intake pipe as an isomeric illustration in the distance-crank angle (distance-time) plane

The 3D-diagrams of EGMF show the back flows within intake pipe perfectly, and so one can find out when and how intensive these back flows occur. The explanation for the back flows can be found, if one analyzes the 2D- and 3D-diagrams of the intake pressure. The 3D-diagrams for the density show a valley (because of the high exhaust gas temperature) when the back flows occur, while the 3D-diagrams of the flow velocity show negative values.

A second back flow could appear when the inlet valve is closing if the cylinder pressure exceeds the intake pipe pressure. The intensity of this second back flow can be captured once again from the 3D-diagrams of EGMF. The 3D-diagrams of the flow velocity and density only confirm these occurrences.

For the gasoline MPI ICE it is useful to have the 3D-diagrams of the flow velocity one's disposal. With its help one can optimize for example the location choice of the gasoline injectors and the intake pipe shape. If supplementary a gasoline spray model is added and as new state variable the gasoline vapor mass fraction is introduced, one can perform this tuning even better

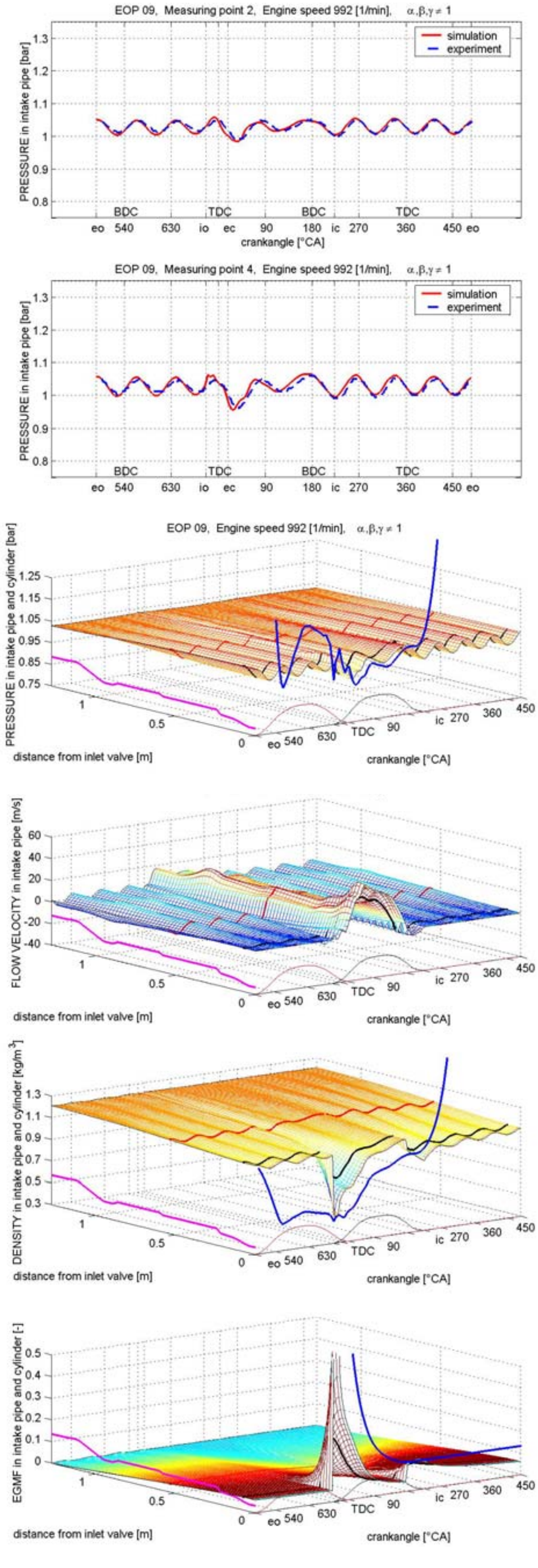

Fig. 8 Results in EOP 09

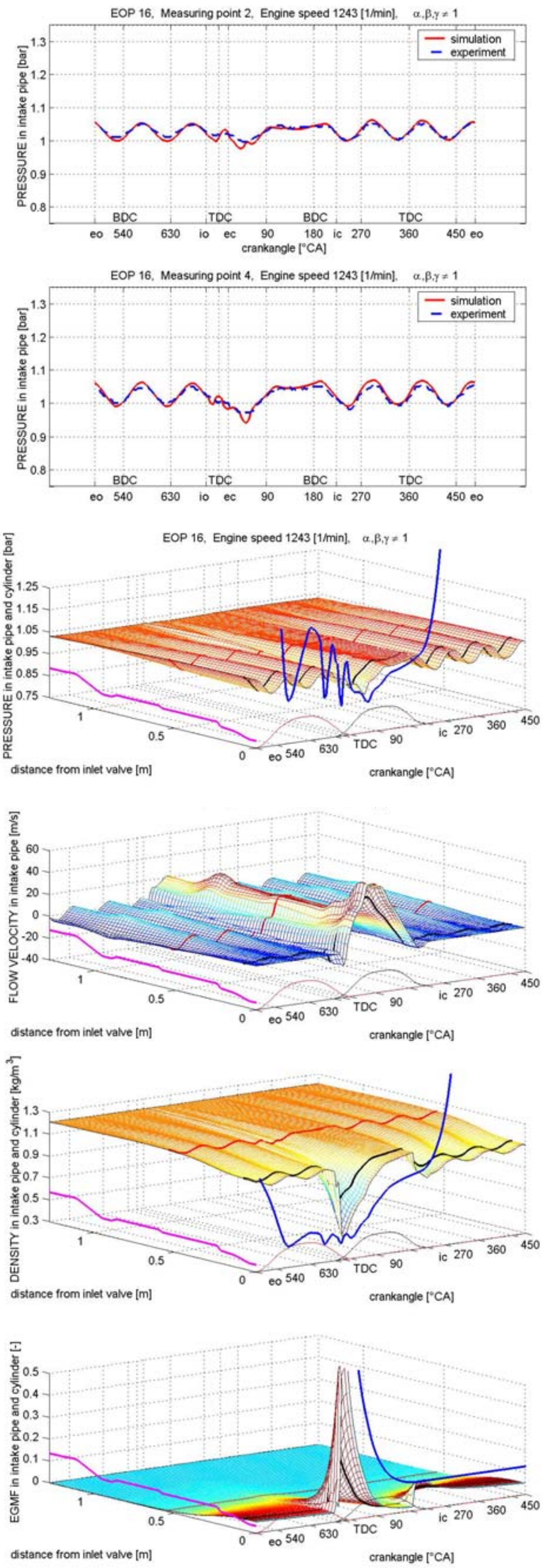

Fig. 9 Results in EOP 16

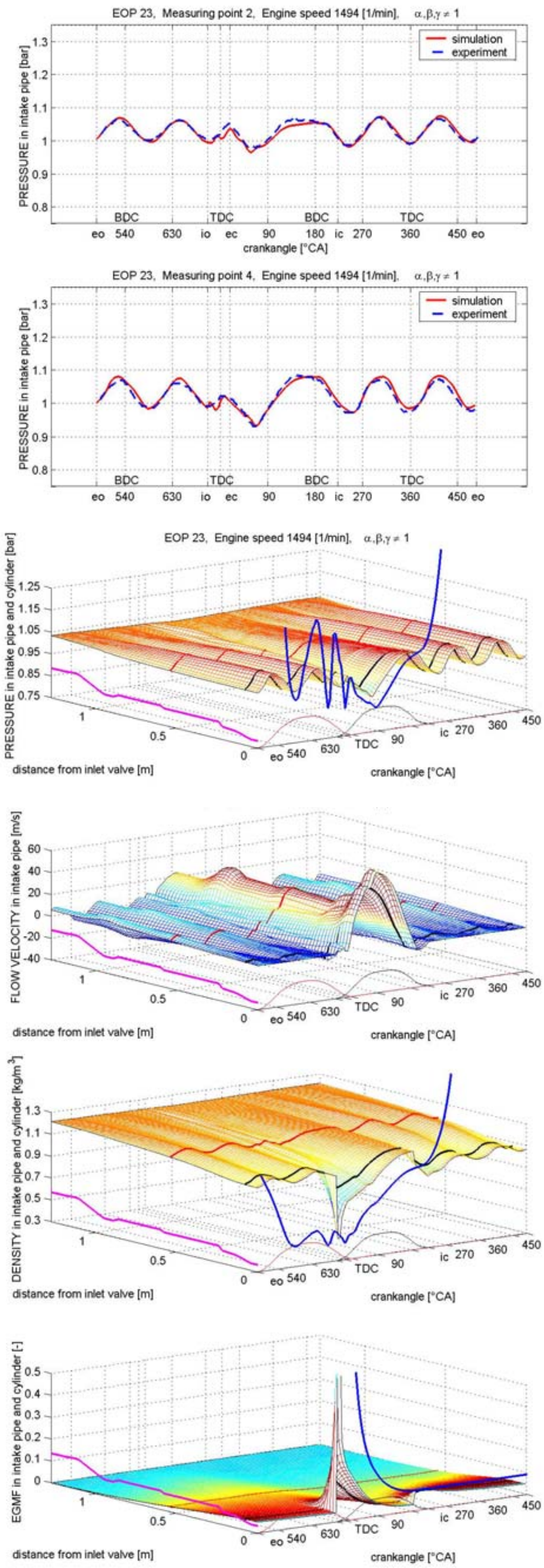

Fig. 10 Results in EOP 23

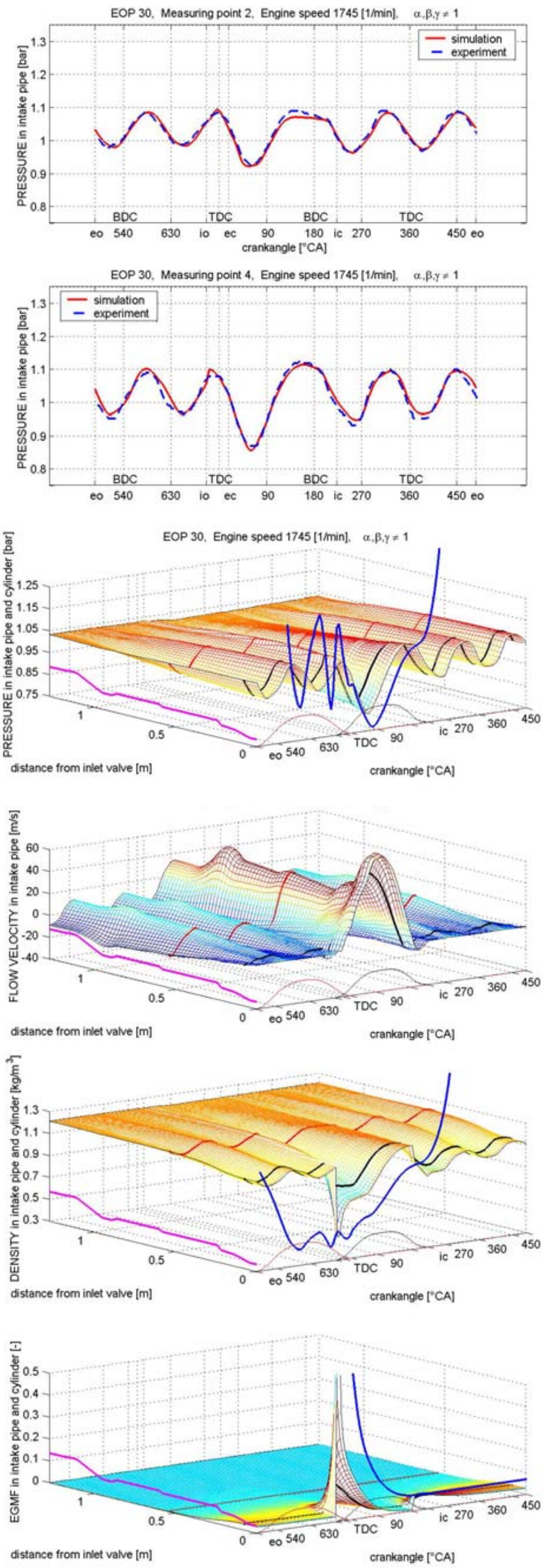

Fig. 11 Results in EOP 30

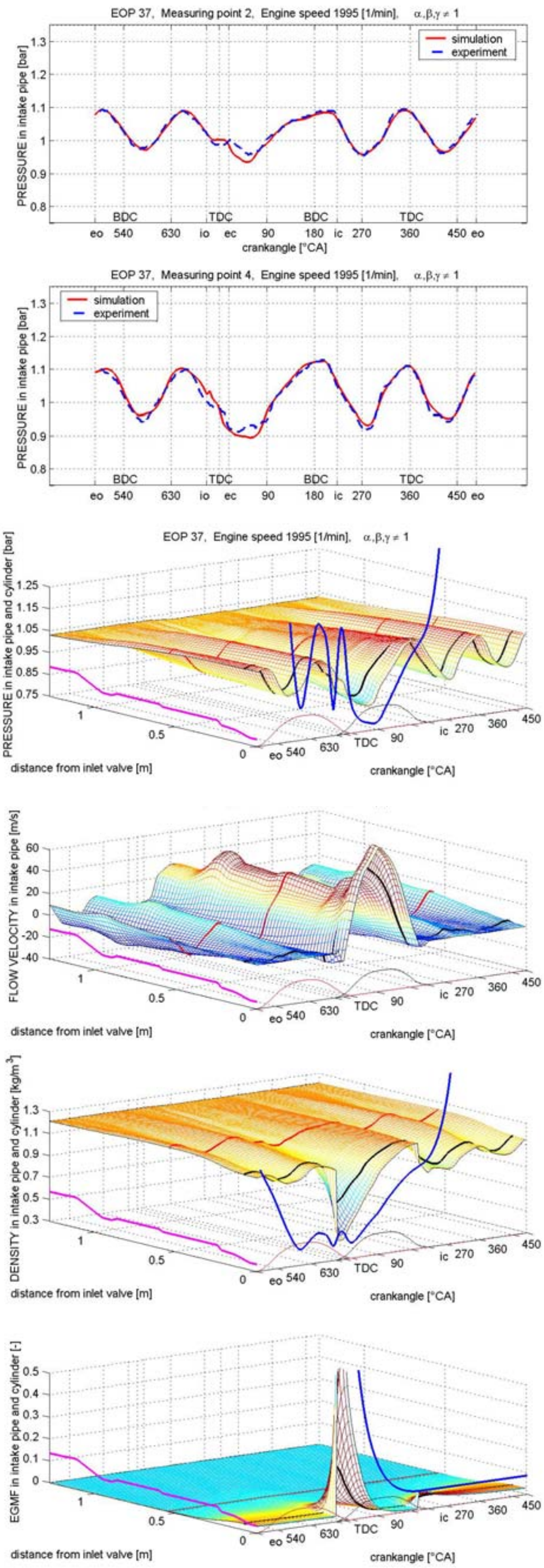

Fig. 12 Results in EOP 37

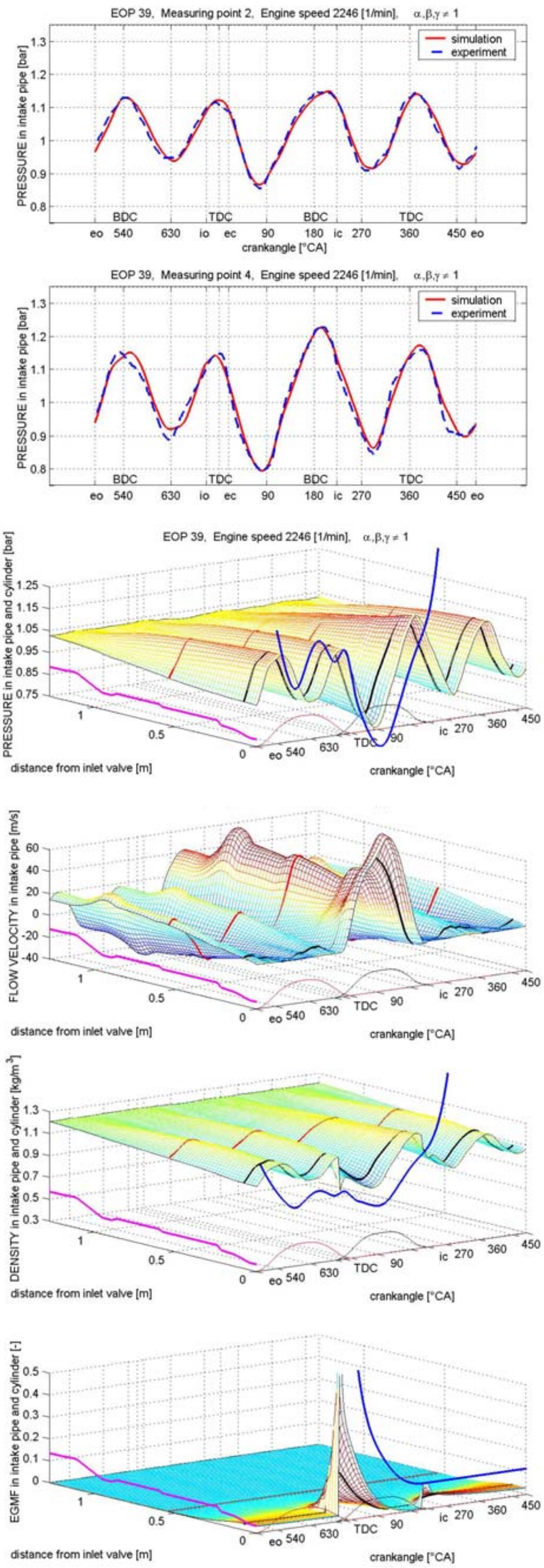

Fig. 13 Results in EOP 39

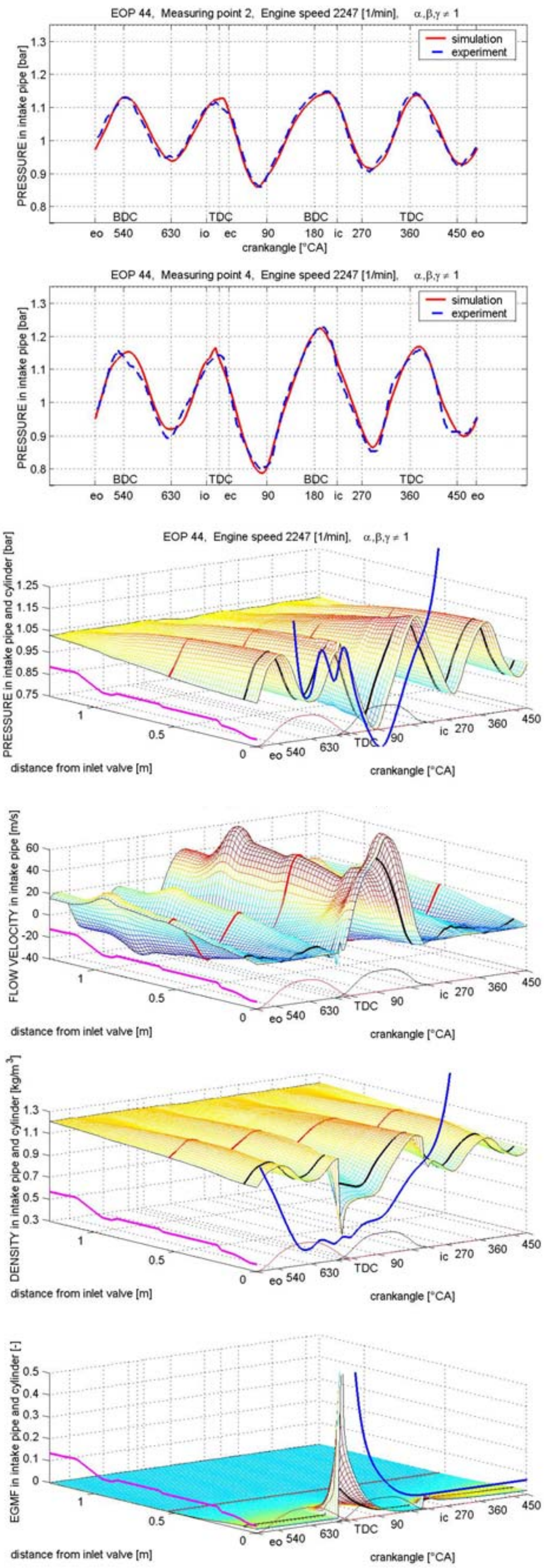

Fig. 14 Results in EOP 44

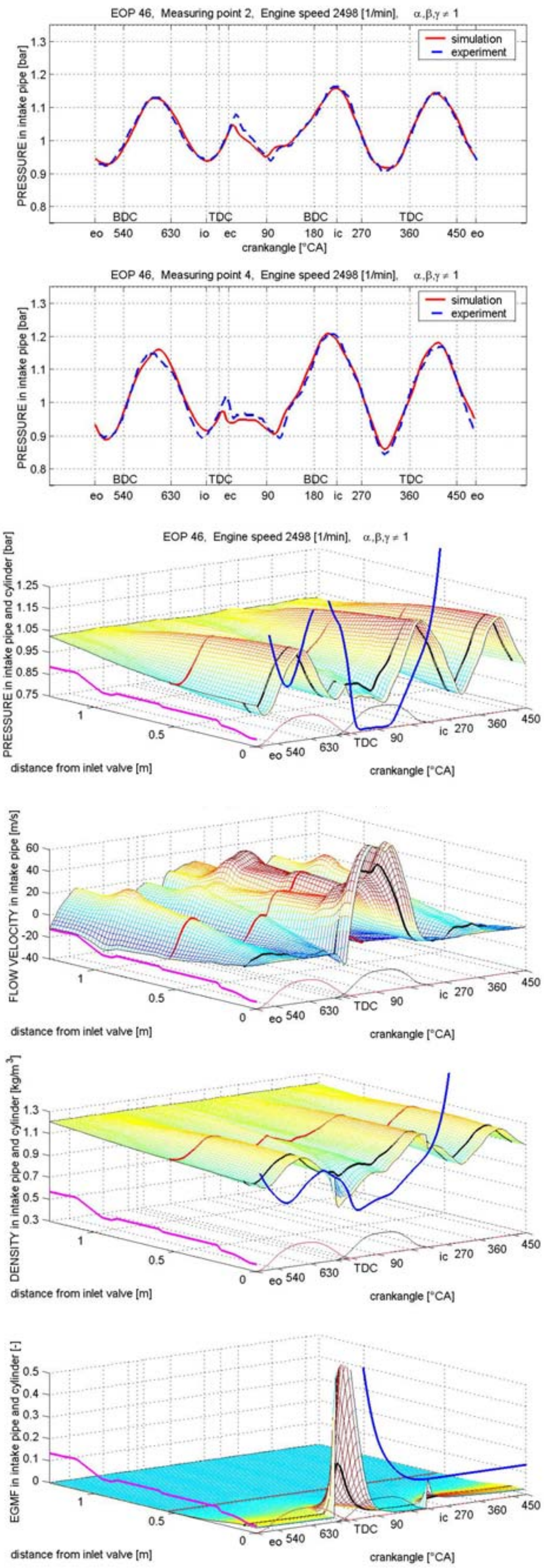

Fig. 15 Results in EOP 46

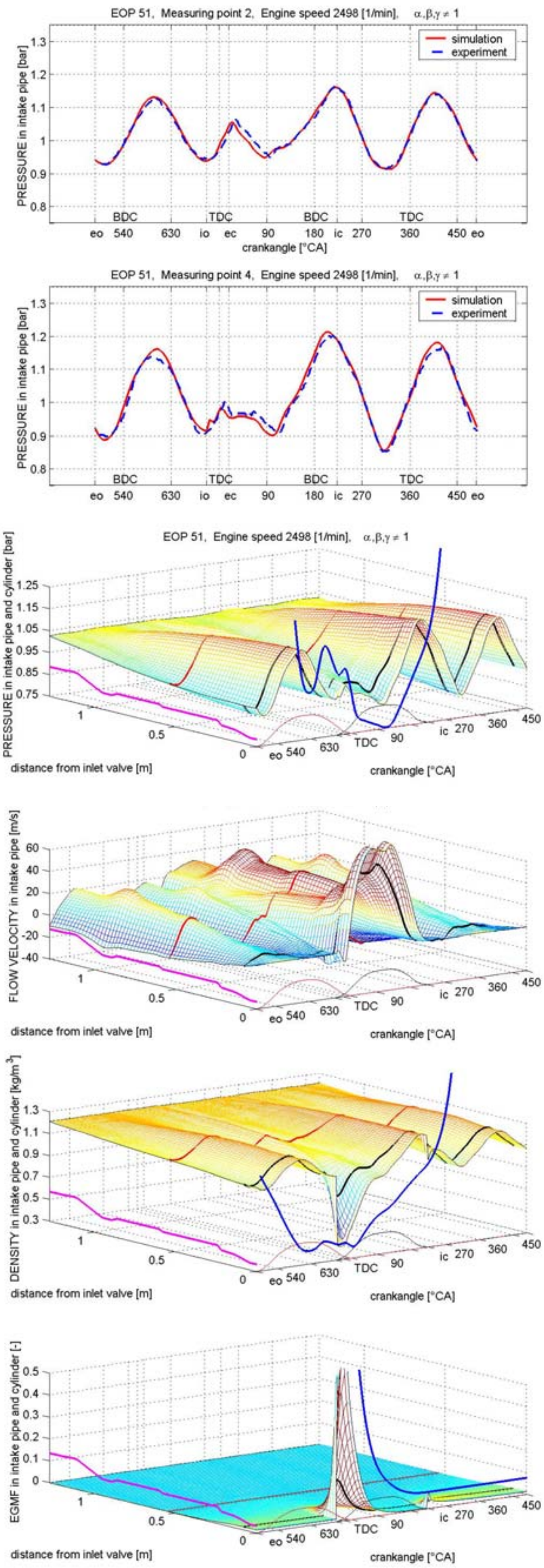

Fig. 16 Results in EOP 51

CONCLUSIONS

The quasi-3D method allows to take into consideration the real distribution of losses along the pipes (as curvatures, asymmetry of the pipes and channels etc). On the contrary, the classical 1D method requires artificial concentration of the distributed losses in some cross sections, which are treated during the simulation as discontinuity interfaces or boundaries [5], [6]. On one hand, the treatment of the boundaries is very time-consuming and causes convergence problems frequently. On the other hand, the simulation results are inaccurate close to the boundaries. This fact becomes more critical because of the complexity of modern manifolds, which requires inserting a series of boundaries along a pipe.

The quasi-3D method is presented here as a compromise between the 1D and true-3D methods witch improves the quality of the 1D-simulation results noticeably, without increasing the cost of computation proportionally.

REFERENCES

[1] Boussinesq, I., *Memoire sur l´influence des frottments dans les mouvements réguliers des fluides*, J. de math. pur et appl., nr. 13, p. 377, (French) 1868

[2] Florea, J., Panaitescu, V., *Mecanica fluidelor*, EDP-Bucuresti (Romanian), 1979

[3] Gheorghiu, V., *Higher Accuracy through Combining of quasi-3D (instead of 1D) with true-3D Manifold Flow Models during the Simulation of ICE Gas Exchange Processes,* SAE Paper 2001-01-1913, Orlando, 2001

[4] Gheorghiu, V., *Quasi-3D Simulation of compressible unsteady flows*, HEFAT, GV1, Victoria Falls, Zambia, 2003

[5] Seifert, H., *Instationäre Strömungsvorgänge in Rohrleitungen an Verbrennungskraftmaschinen*, Springer Verlag (German), 1962

[6] Winterbone, D. E., Pearson, R. J., *Design techniques for engine manifolds - Wave action methods for IC engines*, Professional Engineering Publishing, 1999

[7] Yee, H.-C., *A class of high resolution explicit and implicit shock capturing methods*, Karman Institutes for Fluid Dynamics, Lecture Series 1989-04

[8] Zierep, J., *Grundzüge der Strömungslehre*, Springer Verlag (German), 1997